

Anisotropic Free-Energy Limit of Halos in High-Intensity Accelerators

G. Franchetti and I. Hofmann

GSI Darmstadt, Planckstrasse 1, 64291 Darmstadt, Germany

D. Jeon

Oak Ridge National Laboratory, Oak Ridge, Tennessee 37831

(Received 15 February 2002; published 6 June 2002)

We study halo emittance growth in anisotropic beams and show that the rms emittance growth resulting from mismatch is highly anisotropic, depending on the tune ratio. We find that the free-energy limit calculated by Reiser [J. Appl. Phys. **70**, 1919 (1991)] for an axisymmetric 1D halo can be extended to 2D if understood as an upper bound to the rms emittance growth *averaged per degree of freedom*. The thus-obtained “free-energy limit” of an ideal transport system is compared with the halo rms emittance growth in simulations of the Spallation Neutron Source linac.

DOI: 10.1103/PhysRevLett.88.254802

PACS numbers: 41.75.-i, 29.17.+w, 29.27.Bd

In high-intensity accelerators for protons or ions mismatch of beam envelopes leads to halo formation, which may be a source of beam loss. Most of the halo studies so far have considered round beams with axisymmetric focusing (see the review by Wangler [1]). Some new aspects caused by anisotropy—with the ratio of focusing strengths and/or emittances as additional free parameters—were discussed for 2D [2] and 3D beams [3,4] demonstrating an influence of the mismatch modes on halo size. These studies have shown the strongly increased complexity in halo behavior due to anisotropy and the need for systematic understanding.

In this study we focus on the beam rms properties and show that conversion of free energy from mismatch into rms emittance growth takes place with a significant modification accounting for 2D anisotropy. The 1D issue was first addressed by Reiser [5], who calculated analytically an upper bound to the rms emittance growth of a mismatched axisymmetric beam by assuming complete conversion of the free energy into halo. In 2D such conversion may still happen, but in a pronounced anisotropic way. The detailed conditions are determined in this Letter by carrying out extended parameter studies with the 2D particle-in-cell simulation code MIMAC [6] using a constant focusing transport system with 50 000 simulation particles on a 128×128 grid with self-consistent space charge calculation. Phase space distributions are constructed in 4D phase with the help of the dimensionless invariant $G \equiv A_x^2/\epsilon_x + A_z^2/\epsilon_z$, by using the invariants $A_{x,z}^2$ in action-angle variables for the equivalent uniform beam as defined in Ref. [7]. Phase-space truncation of the normalized Gaussian at $n\sigma_G$ is understood as $\exp -G/2$ discarding all particles for which G exceeds $n(\sigma_G = 1)$, and renormalizing to rms equivalence. Obviously such a distribution is only rms matched since space charge forces are not linear. As a first example, we consider in Fig. 1 a beam with weak space charge, equal emittances in the two transverse directions, z and x , and define the rms emittance growth as the ratio of final to initial rms emittance. The tune depres-

sion in x is assumed to be $k_x/k_{0x} = 0.95$, which is typical for high-current rings. The tune ratio, k_z/k_x , is scanned from 0.9 to 1.1 in small steps, which includes the region of maximum growth. Each marker indicates a simulation run over 190 betatron periods, which is found sufficient to reach practically saturation of the rms emittance growth effect. The mismatch factor, defined as the ratio of mismatched to matched envelopes, is chosen equal for both

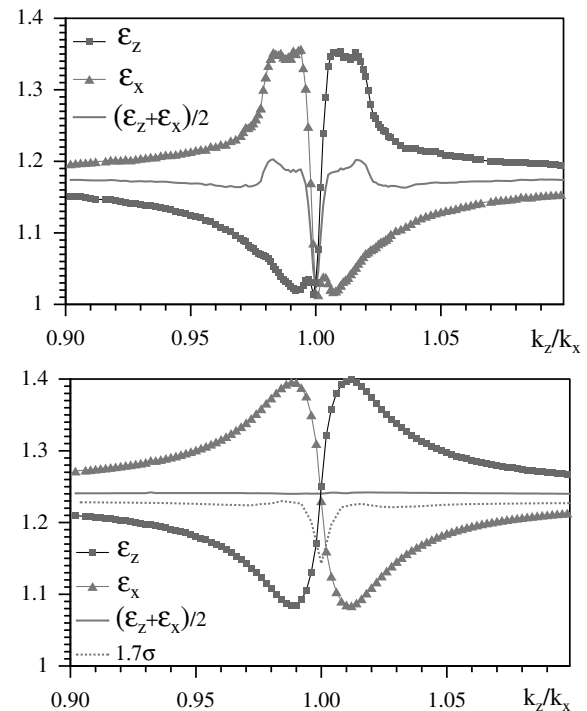


FIG. 1. Final rms emittance growth factors in z , x , and averaged over z and x as a function of tune ratio k_z/k_x ($k_x/k_{0x} = 0.95$, $\epsilon_z/\epsilon_x = 1$, and $M = 1.4$) for waterbag (top) and untruncated Gaussian (bottom) distributions; averaged growth factor also for Gaussian with truncation at $1.7\sigma_G$ (dotted line, bottom graph).

directions ($M = M_z = M_x$) with zero derivatives. This choice excites both envelope modes, except for $k_x = k_z$.

The rms emittance growth curve of the waterbag (WB) beam has a pronounced minimum at tune ratio unity, where the breathing mode of axisymmetric beams is excited [1]. It rises steeply in the direction for which the focusing strength increases, i.e., in z for $k_z/k_x > 1$, and in x for $k_z/k_x < 1$. The Gaussian shows a much smoother but similarly pronounced anisotropic response. Surprisingly, $\epsilon_z + \epsilon_x$ is found constant at 24%, to within less than $\pm 0.2\%$ variation. We interpret this with the observation that each emittance is proportional to the square of the velocity spread (divided by the tune), hence energy, and the sum to the total energy. Comparing this value with the analytical expression in Reiser's model for axisymmetric beams [5], we find better than 1% agreement. For axisymmetric beams such nearly 100% conversion—somewhat less for higher space charge—was already shown by Cucchetti *et al.* [8]. To explore the role of the Gaussian tails in phase space we have compared results with phase-space truncation at different $n\sigma_G$: at $3\sigma_G$ the response curve is practically unchanged; truncation below $2\sigma_G$ leads, however, to a dip at $k_z/k_x = 1$ and reduced conversion (see example with $1.7\sigma_G$ in Fig. 1), while the WB result is approached by truncating down to a small fraction of σ_G .

We use the fact that the *averaged* growth factor is independent of k_z/k_x to plot it as a function of M and find overall agreement with Reiser's theoretical curve (Fig. 2). We also show the maxima and minima of growth factors found in the interval $0.9 < k_z/k_x < 1.1$. The pronounced anisotropy of the response is in contrast with a simple picture of thermalization and should be seen as the result of the underlying resonance behavior. The WB rms emittance growth in Fig. 1 remains everywhere below that of the Gaussian, but the maximum anisotropy is similar.

The anisotropic response can be understood in terms of the distance of fixed points of the 2:1 resonance from the beam core, expressed as a function of the tune ratio. Particles are caught into a resonance with mismatch modes of frequency $\omega_{1,2}$ if this frequency is sufficiently close to

twice the betatron frequency. ω_1 (fast mode) and ω_2 (slow mode) result from the exact dispersion relation for envelope eigenfrequencies of anisotropic beams (see, for instance, Ref. [9]). The spectrum of possible single particle betatron frequencies for the matched beam ranges from the space charge depressed values k_z, k_x inside the core to the zero-current values, k_{0z}, k_{0x} , for infinite betatron amplitudes. By calculating numerically the dependence of k_z (k_x) on amplitude for oscillations along the z (x) axis we obtain the distance of resonant amplitudes from the core. These fixed points are shown in Fig. 3 in units of matched beam radii.

For the breathing mode resonance the fixed point is always farther away from the core than for the quadrupolar one. It is found at 1.73 core radii (or 3.46 real space σ 's) for symmetric focusing, which agrees with Ref. [1]. For the WB beam, with a sharp real space edge at 2.45σ , this leads to the only few percent rms emittance growth for a pure breathing mode. Phase-space truncation of the Gaussian at $1.7\sigma_G$ extends the edge to 2.63σ in real space and enhances the growth visibly; the full Gaussian tails populate most effectively the breathing mode resonance and we assume that this leads to the complete conversion in Fig. 1. For $k_z/k_x < 1$ the fixed points of the z motion for resonance with either mode move away. The fixed points pertaining to the x motion, instead, approach the core. This enhances the space charge coupling force, and we use this to explain why ϵ_x grows predominantly. The x -halo enhancement in this region can be described in terms of resonance overlap as was pointed out by Ikegami [2]; this ceases below $k_z/k_x = 0.984$, where the quadrupolar mode fixed point drops into the core, hence no effective amplitude gain—see the visible drop in ϵ_x in Fig. 1 for the WB. For $k_z/k_x = 0.968$ the breathing mode fixed point with the z motion is at infinity. For k_z/k_x above unity the picture is mirrored, with z and x interchanged. Also shown in Fig. 3 is M_r , the ratio of amplitudes of the quadrupolar mode to the breathing mode under the assumption of $M_z = M_x$, which approaches unity for k_z/k_x sufficiently

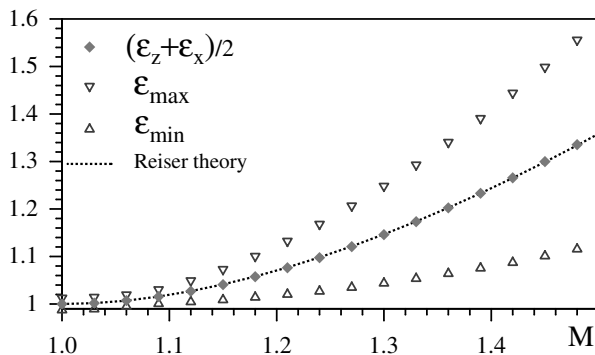


FIG. 2. Maximum, minimum, and averaged rms emittance growth factors compared with Reiser theory, as a function of M for Gaussian beams ($\epsilon_z/\epsilon_x = 1, k_x/k_{0x} = 0.95$).

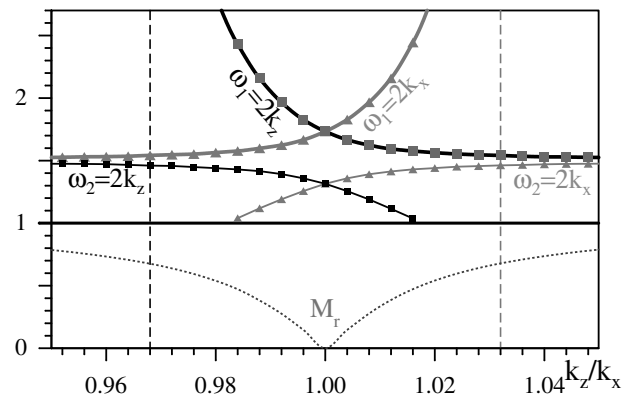


FIG. 3. Distance of fixed points from core (in units of beam radii) for resonance with eigenmodes; M_r amplitude ratio for $M_z = M_x$.

different from 1. Both the migration of fixed points with tune ratios and the change of M_r contribute to the strongly asymmetric emittance growth of Fig. 1.

Curves for stronger space charge, pertinent to linacs, show similar features of anisotropic growth. The main difference is that the peaks right and left to $k_z/k_x = 1$ are farther apart, according to the increased tune shift, and less time is needed to get saturation of the growth, while the maximum emittance growth increases only weakly with space charge. As an example we show in Fig. 4 a scan for $k_x/k_{0x} = 0.6$ and $M = 1.3$, which reveals two peaks as in Fig. 1 for both distributions. We have found that the mismatch enhanced anisotropy and the average rms emittance growth as a function of M follow a similar pattern as in Fig. 2 due to a similar distribution of fixed points over a broader span in k_z/k_x .

The increased peak separation is consistent with the analytical result that the quadrupolar mode fixed points drop into the core at tune ratios 0.7 and 1.26. The resulting anisotropy exceeds only slightly that for weaker space charge. Additional emittance growth in z is identified in two major bands between $0.2 \lesssim k_z/k_x \lesssim 0.5$. They need to be taken into account for linac applications with correspondingly weak longitudinal focusing and are not associated with the usual 2:1 parametric resonance, but with higher order mode resonances. Candidates are the fourth order resonances leading to equipartitioning in matched beams [10], with a modification due to the time depen-

dence of the driving slow mode ($2k_z - 2k_x \approx \omega_2$), or purely z growth by $4k_z \approx \omega_2$. For the $3.4\sigma_G$ Gaussian (practically full Gaussian) the average emittance growth in z and x at $k_z/k_x = 1$ results as 19%, which is below the prediction of 23% from Reiser's analytical model for $M = 1.3$. The weak gradient of the averaged emittance response with respect to k_z/k_x is attributed to the gradient in k_z/k_{0z} due to constancy of k_x/k_{0x} . As above the fine structure in the k_z/k_x dependence of the WB case is largely smoothed out by Gaussian tails; for the $1.7\sigma_G$ Gaussian it reappears as a result of tail truncation. Reiser's analytical expression can again be used as an estimate for the upper bound of anisotropic emittance growth *averaged per degree of freedom*: this is fully justified for $0.5 < k_z/k_x < 1.5$, but also roughly for the larger range $0.2 < k_z/k_x < 1.5$. This "ideal" limit will be compared below with the "realistic" growth in linac design, where nonsmooth design, rapidly changing parameters, and transitions in structures can give rise to further growth.

A remark on equipartition may be appropriate here. The energy anisotropy is given by the ratio $\epsilon_z k_z / \epsilon_x k_x$; hence it is initially proportional to the tune ratio in our examples. Figure 4 shows that below $k_z/k_x = 1$ the emittance growth due to mismatch occurs primarily in the x direction, where the beam is initially "hotter"; hence it is pushed away from equipartition; only in the two resonance bands encountered below $k_z/k_x \approx 0.5$ the effect of mismatch goes into the direction of equipartition. Moreover, the $3.4\sigma_G$ Gaussian distribution, which is practically in "thermal equilibrium" at $k_z/k_x = 1$, is not less subject to emittance growth from mismatch than the nonequipartitioned cases for different k_z/k_x . This finding is relevant for proposals which employ beams in thermodynamic equilibrium for linac design [11].

We have also checked results (of WB beams) for mismatch factors different in z and x , but keeping constant the rms value $M_{\text{rms}}^2 \equiv \frac{1}{2}(M_z^2 + M_x^2)$ as a tentative ansatz to normalize the mismatch on the basis of single particle harmonic oscillator energy. For the case studied, $M_{\text{rms}} = 1.3$, emittance profiles are found more asymmetric compared with Fig. 4; but the maximum emittance increase in the interval $0.5 < k_z/k_x < 1.5$ of 32% for equal mismatch now varies between 27% and 37% in the region $1.1 < M_x < 1.5$. This indicates that the free-energy limit depends primarily on the *average* mismatch factor M_{rms} .

We suggest that the 2D results are relevant for comparison with the halo in high intensity linacs if we relate z to the longitudinal, and x to either one of the transverse coordinates x, y . As an example, we consider the Spallation Neutron Source (SNS) linac, which is designed for 2 MW of 1 GeV H^- , with a drift tube linac (DTL) from 2.5 to 85 MeV and a coupled cavity linac up to 180 MeV followed by the superconducting linac [12]. The high power requires careful control of emittance blowup and beam halo, primarily in the transverse direction. We

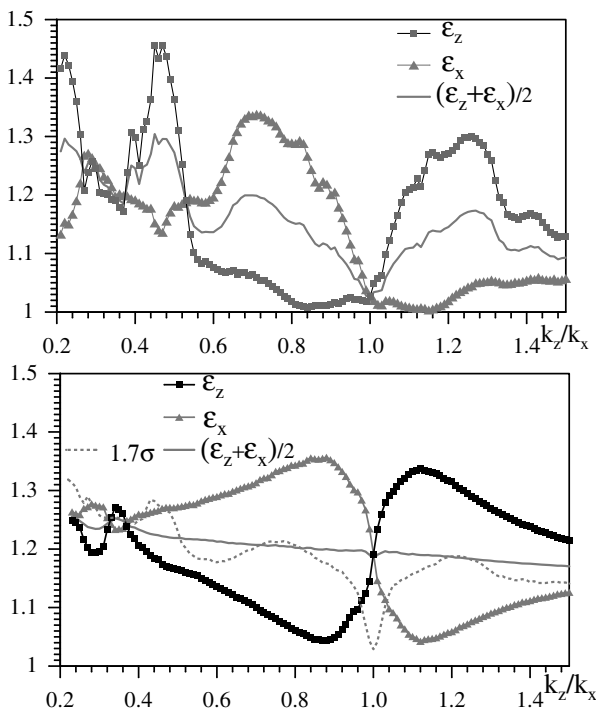


FIG. 4. Rms emittance growth factors (after 95 betatron periods) for WB (top) and $3.4\sigma_G$ Gaussian (bottom) with $k_x/k_{0x} = 0.6$, $\epsilon_z/\epsilon_x = 1$ and $M = 1.3$; averaged growth also for $1.7\sigma_G$ Gaussian.

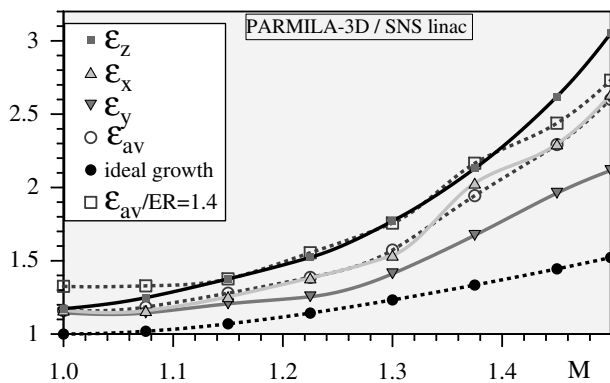


FIG. 5. Emittance growth factors for the SNS linac design for the nominal case ($\epsilon_z/\epsilon_x = 1$) compared with the ideal growth; averaged growth also for the increased initial emittance ratio ($\epsilon_z/\epsilon_x = 1.4$).

have checked the rms halo by 3D PARMILA [13] simulations using a WB input distribution into the DTL with 100 000 particles and as nominal case: 38 mA current, transverse normalized emittances $\epsilon_{x,y} = 0.02$ cm mrad and $\epsilon_z/\epsilon_{x,y} = 1$ (typical $k_x/k_{0x} \approx 0.6$). We find that k_z/k_x drops from near unity in the early part of the DTL to values as low as 0.3 at the end of it, while jumping above and below unity in the superconducting part. The conversion of mismatch free energy into rms emittance growth is found to take place over the full length of the linac, which corresponds to only 17 betatron periods (defined without space charge). Hence, this design has a wide range of k_z/k_x , and thus it would be expected that the mechanisms indicated in Fig. 4 (including the peak near tune ratio 0.5) should be present—though not easily distinguishable—and would cause conversion of a large fraction of mismatch free energy into rms emittance growth distributed over *all three* planes, where it should be noted that *two* transverse degrees have to share the longitudinal energy. This distributed emittance growth is reflected by the graphs in Fig. 5 and compared with the ideal growth per degree of freedom based on Reiser's 2D model (a more adequate comparison with the ideal growth from a 3D model is left to future work). The presence of $\approx 16\%$ average rms emittance growth (15% in x, y and 17% in z) without mismatch is a result of practical constraints in a specific linac. The further growth by mismatch follows a trend, which can be qualitatively compared with the parabolic law $1 + \alpha(M - 1)^2$ typical for free-energy conversion: we find that $\alpha \approx 4$ in $1.1 < M < 1.3$. This is 60% higher than the ideal growth corresponding to $\alpha \approx 2.5$ —presumably due to the nonadiabatic behavior of the rapidly changing linac structure. We also indicate the result for an initial ϵ_z increased by 40%. A similar dependence on M is found: the average growth factor, $(\epsilon_z + \epsilon_x + \epsilon_y)/(3 \times 0.02$ cm mrad), increases by not more than 15%–20% for all values of M . The enhancement of the growth of $\epsilon_{x,y}$ for $M = 1$ from 15% to 26% results from nonequipartition on the fourth order

coupling resonance stop band $2k_z - 2k_x \approx 0$ explored in more detail in Refs. [10,14,15]. We note that if a design were chosen with k_z/k_x everywhere close to 0.7, it could be inferred from Fig. 4 that emittance growth should predominantly occur in the transverse plane.

In summary, anisotropy adds a number of new features to the discussion of mismatch induced halo: growth of the rms emittance can be very sensitive to k_z/k_x due to the motion of stable fixed points for the parametric resonance and due to the appearance of fourth order resonances; beams may be driven away from initial equipartition, but Reiser's free-energy model is still applicable if modified; with respect to real accelerators our emittance growth results may be seen as a lower limit, which practical design could try to reach within the constraint that such efforts may have to be balanced against cost.

The authors gratefully recognize comments and suggestions by R. A. Jameson on linac design and by M. Reiser on free energy. The hospitality and support of the SNS Project Office and of the AGS Division and CDIC at Brookhaven National Laboratories during part of the work are acknowledged by two of the authors (I. H. and G. F.).

-
- [1] T. P. Wangler, Phys. Rev. ST Accel. Beams **1**, 084201 (2000).
 - [2] M. Ikegami, Nucl. Instrum. Methods Phys. Res., Sect. A **454**, 289 (2000).
 - [3] R. L. Gluckstern, A. V. Fedotov, S. Kurennoy, and R. Ryne, Phys. Rev. E **58**, 4977 (1998).
 - [4] A. V. Fedotov, R. L. Gluckstern, S. S. Kurennoy, and R. D. Ryne, Phys. Rev. ST Accel. Beams **2**, 014201 (1999).
 - [5] M. Reiser, J. Appl. Phys. **70**, 1919 (1991).
 - [6] G. Franchetti, I. Hofmann, and G. Turchetti, in *Workshop on Space Charge Physics in High Intensity Hadron Rings, Shelter Island, New York, 1998*, edited by A. U. Luccio and W. T. Weng, AIP Conf. Proc. No. 448 (AIP, Woodbury, NY, 1998), p. 233.
 - [7] M. Reiser, *Theory and Design of Charged Particle Beams* (Wiley, New York, 1994), p. 342 ff.
 - [8] A. Cucchetti, M. Reiser, and T. P. Wangler, in *Proceedings of the Particle Accelerator Conference, San Francisco, 1991* (IEEE, Piscataway, NJ, 1991), p. 251.
 - [9] I. Hofmann, Phys. Rev. E **57**, 4713 (1998).
 - [10] I. Hofmann, G. Franchetti, O. Boine-Frankenheim, J. Qiang, R. Ryne, D. Jeon, and J. Wei, in *Proceedings of the Particle Accelerator Conference Chicago, 2001*, edited by Y. Cho (IEEE, Piscataway, NJ, 2001).
 - [11] M. Reiser and N. Brown, Phys. Rev. Lett. **74**, 1111 (1995).
 - [12] J. Stovall *et al.*, in *Proceedings of the Particle Accelerator Conference Chicago, 2001* (Ref. [10]).
 - [13] H. Takeda, LANL Report No. LA-UR-98-4478, Los Alamos, 1999 (unpublished).
 - [14] I. Hofmann, J. Qiang, and R. Ryne, Phys. Rev. Lett. **86**, 2313 (2001).
 - [15] I. Hofmann and O. Boine-Frankenheim, Phys. Rev. Lett. **87**, 034802 (2001).